The 2016 World Congress on
The 2016 Structures Congress (Structures16)
Jeju Island, Korea, August 28-September 1, 2016

Mode Identifiability of a Cable-Stayed Bridge using Modal Contribution Index

*Tian-Li Huang[1)] and Hua-Peng Chen[2)]

[1)] *School of Civil Engineering, Central South University, Changsha, Hunan Province, 410075, China*
[1), 2)] *Department of Engineering Science, University of Greenwich, Chatham Maritime, Kent, ME4 4TB, UK*
[1)] *htianli@csu.edu.cn*
[2)] *h.chen@gre.ac.uk*

(Received , Revised , Accepted)

Abstract. The modal identification of large civil structures such as bridges under the ambient vibrational conditions has been widely investigated during the past decade. Many operational modal analysis methods have been proposed and successfully used for identifying the dynamic characteristics of the constructed bridges in service. However, there is very limited research available on reliable criteria for the robustness of these identified modal parameters of the bridge structures. In this study, two time-domain operational modal analysis methods, the data-driven stochastic subspace identification (SSI-DATA) method and the covariance-driven stochastic subspace identification (SSI-COV) method, are employed to identify the modal parameters from field recorded ambient acceleration data. On the basis of the SSI-DATA method, the modal contribution indexes of all identified modes to the measured acceleration data are computed by using the Kalman filter, and their applicability to evaluating the robustness of identified modes is also investigated. Here, the benchmark problem, developed by Hong Kong Polytechnic University with field acceleration measurements under different excitation conditions of a cable-stayed bridge, is adopted to show the effectiveness of the proposed method. The results from the benchmark study shows that the mode identifiability may depend on not only the ambient excitation intensity but also the modal contributions to the measured vibration data. A critical value of modal contribution index of 2% for a reliable identifiability of modal parameters is then suggested for the benchmark problem.

Keywords: Cable-stayed bridge; operational modal analysis; dynamic characteristics; modal contribution index; ambient vibration response

1. Introduction

The structural modal properties such as the frequencies, damping ratios and mode shapes are often used for design validation, finite element model updating and damage assessment of the civil engineering structures such as bridges. These modal properties should be determined in normal operational conditions to represent real dynamic response of the structures. There are two methods to obtain the modal properties, i.e., the experimental modal analysis (EMA) method and the operational modal analysis (OMA) method. The traditional EMA methods need both the input (excitation) and output (response) measurements to estimate the modal parameters. Many EMA algorithms have been developed such as the Single-Input/Single-

[1)] Associate Professor
[2)] Professor

Output (SISO), Single-Input/Multi-Output (SIMO) and Multi-Input/Multi-Output (MIMO) techniques in time domain and frequency domain [1]. However, the EMA methods may not be suitable for identifying the modal properties of large civil engineering structures under operational condition due to the difficulty in the acquirement of the excitation. The OMA method, also called as ambient excitation or output-only modal analysis method, has drawn great attention in civil engineering community, since it only uses the response measurements of the structures in operational condition subjected to ambient excitation for identifying the dynamic characteristics.

Over the past two decades, several OMA methods have been proposed, including the peak-picking (PP) method [2], the frequency domain decomposition (FDD) method [3] and the poly-reference least squares complex frequency domain (p-LSCF) method [4] in the frequency domain, the Eigen-system realization algorithm (ERA) method [5], and the stochastic subspace identification (SSI) method [6-7] in the time domain. These OMA methods have been successfully applied to many real bridges, such as the Vasco da Gama cable-stayed bridge [8], the Qingzhou cable-stayed bridge [9], the Infante D. Henrique Bridge [10], and Humber Bridge [11]. Moreover, the modal parameters of some specific structures can also be obtained by other methods proposed in studies [12-14]. The identified modal parameters can then be utilised for many applications, such as finite model updating [15-16] and structural damage assessment [17-18].

However, these identified modal parameters are often obtained by relatively small amplitudes of structural response due to normal wind and traffic excitation. In certain extreme circumstances, even some lower-order mode shapes are not able to be reliably identified from the ambient responses under weak excitations [19]. The issue how to quantitatively judge the robustness of these identified modal characteristics is still not well understood and even rarely investigated. There is no theoretical or even empirical criterion available for the confidence of the identified modal parameters. In order to investigate the issue, Ni et al. (2015) [19] investigated the identifiability on the second mode of the Ting Kau Bridge (TKB) which is deficient under various weak wind conditions by using the data-driven stochastic subspace identification (SSI-DATA) method. It is concluded that the threshold of wind speed for reliable identification this deficient mode is 7.5m/s. Therefore, a benchmark problem on the mechanism study of mode identifiability and robustness of a cable-stayed bridge using the monitored data from the instrumented Ting Kau Bridge under different excitation conditions has been developed. Recently, the results for the benchmark problem on the modal identifiability of the cable-stayed bridge are reported in many studies [20-23].

In this paper, two time-domain OMA methods, e.g. the data-driven stochastic subspace identification (SSI-DATA) method and the covariance-driven stochastic subspace identification (SSI-COV) method, are adopted to identify the modal parameters from ambient acceleration measurements for the benchmark problem,. Based on the SSI-DATA method, the modal contribution indexes of all identified modes to the measured vibration data are computed by using the Kalman filter, and their feasibility to evaluate the robustness of identified modes is investigated. The results show that the mode identifiability may depend on not only the ambient excitation intensity but also the modal contributions to the measured vibration data. A critical value of modal contribution index for a reliable and robust identification of modal parameters is then suggested.

2 Benchmark problem on modal identifiability

2.1 Description of Ting Kau Bridge and SHM system

The Ting Kau Bridge (TKB) shown in Figs.1 and 2, located in Hong Kong, is a three-tower cable-stayed bridge connecting the Tsing Yi and Ting Kau. The total length of Ting Kau Bridge

is 1177m including two main spans of 448m and 475m, respectively, and two side spans of 127m each. The heights of three main towers are 170m (Ting Kau Tower), 194m (Central Tower) and 158m (Tsing Yi Tower), respectively. The width of the bridge deck is 42.8m, consisted of two separated carriageways with a width of 18.8m each and a 5.2m gap. The two carriageways are connected with cross-girders with 13.5m interval. The cable system has four planes with a total of 384 stay cables supporting the bridge decks. The unique stabilising cables were adopted in the bridge for enhancing the stability of the three main towers. It includes eight longitudinal stabilising cables diagonally connecting the top of the central tower to the side towers and 64 transverse stabilising cables that are used to restrain the three main towers in the transverse direction.

Fig. 1 The Ting Kau Bridge

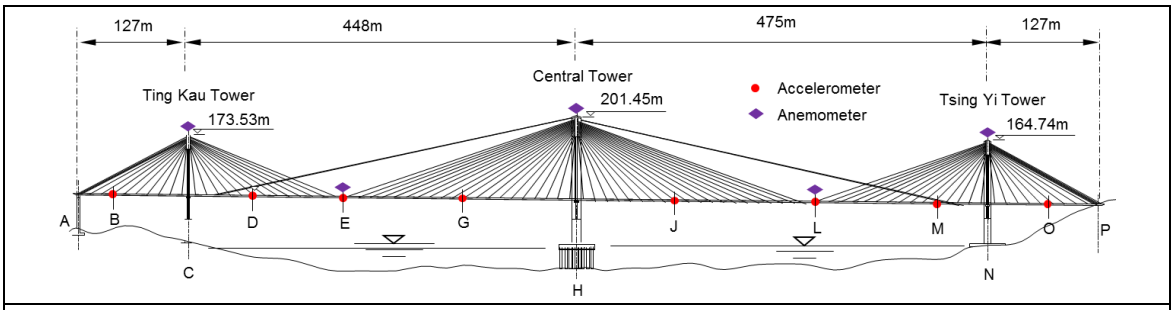

Fig. 2 Deployment of accelerometers and anemometers on Ting Kau Bridge

A structural health monitoring (SHM) system with more than 230 sensors has been permanently installed on the TKB after its complete construction in 1999 [24]. The sensors installed on the bridge include accelerometers, anemometers, strain gauges, anemometers, displacement transducers, temperature sensors and weigh-in-motion sensors [25]. As illustrated in Fig. 2, there are 3 anemometers installed at the top of the three main towers and 4 anemometers installed at the both sides of the sections E and L of the bridge deck. The sampling frequency of these anemometers is 2.56 Hz. In addition, there are 24 uni-axial accelerometers permanently installed at eight sections (B, D, E, G, J, L, M, O) of the bridge deck. The detailed deployment of these 24 accelerometers on the bridge deck is shown in Fig. 3. The accelerometers (1, 3, 4, 6, 7, 9, 10, 12, 13, 15, 16, 18, 19, 21, 22, 24) installed on both sides of the bridge deck measure the vertical accelerations, and the accelerometers (2, 5, 8, 11, 14, 17, 20, 23) installed along the middle of the bridge deck collect the transverse acceleration measurements. The sampling frequency of these accelerometers is 25.6Hz. Only the data collected from these sensors in various operation conditions are adopted in the present

benchmark study.

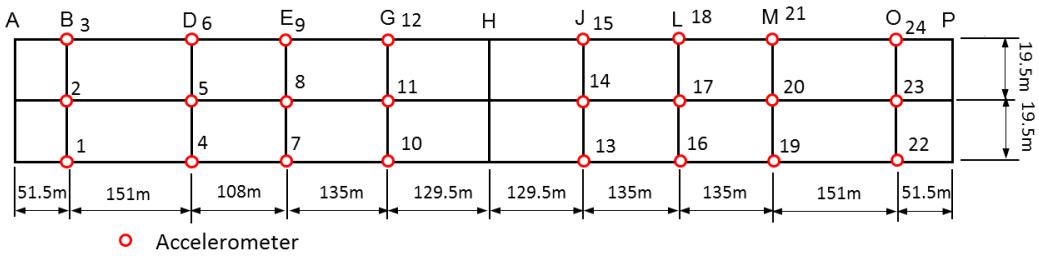

Fig. 3 Detailed deployment of 24 accelerometers on bridge deck

Table 1 Total 19 data samples under different wind conditions provided by benchmark study

Wind Condition	Sample	Time duration	Mean hourly wind speed (m/s)	Note
Weak wind	S1	15:00-16:00, 28 Dec 1999	2.00	
	S2	15:00-16:00, 18 Feb 1999	3.40	
	S3	15:00-16:00, 01 Mar 1999	3.34	
	S4	15:00-16:00, 21 Jun 1999	3.41	
	S5	15:00-16:00, 24 Jul 1999	6.17	
	S6	15:00-16:00, 12 Aug 1999	4.20	
Typhoon	S7	03:00-04:00, 07 Jun 1999	12.11	Maggie
	S8	02:00-03:00, 23 Aug 1999	15.62	Sam
	S9	06:00-07:00, 16 Sep 1999	21.72	York1
	S10	15:00-16:00, 16 Sep 1999	15.91	York2
Critical (wind speed around 7.5m/s)	S11	08:00-09:00, 07 Jun 1999	7.36	7-Jun
	S12	22:00-23:00, 16 Sep 1999	7.77	16-Sep
	S13	09:00-10:00, 26 Sep 1999	7.43	26-Sep
Unknown	S14	1 hour	unknown	Acc1
	S15	1 hour	unknown	Acc2
	S16	1 hour	unknown	Acc3
	S17	1 hour	unknown	Acc4
	S18	1 hour	unknown	Acc5
	S19	1 hour	unknown	Acc6

2.2 Description of field measurement records

In the present benchmark study on mode identifiability, a total of 13 data samples of acceleration measurements collected from these 24 accelerometers with known wind conditions are listed in Table 1. The duration of these acceleration data samples is 1 hour and these data were recorded in 1999. As shown in Table 1, these data samples can be classified into three groups i.e. weak wind, typhoon and critical wind speed (around 7.5m/s), depending on the mean hourly wind speed calculated from the anemometers installed on the bridge deck. In addition, 6 more data samples of acceleration records collected from the same accelerometers with unknown wind conditions are provided as blind data, as listed in Table 1.

The duration of these data samples is also 1 hour and their record times are unknown. These blind data samples include 2 data samples under weak wind condition, 2 data samples under typhoon condition and 2 data samples under wind speed around 7.5m/s. These blind data samples are utilised to verify the results by using the OMA methods and the proposed indexes for determining the robustness of identified modes in this paper.

3. Operational modal analysis using SSI-DATA and SSI-COV

In this study, two time-domain OMA methods, e.g. the data-driven stochastic subspace identification (SSI-DATA) method and the covariance-driven stochastic subspace identification (SSI-COV) method, are employed to extract modal properties such as frequencies and mode shapes from the collected acceleration measurements under different wind speed conditions.

The SSI-DATA technique directly adopts time domain data, without requiring the transfer of the measured data into correlations or spectra. On the other hand, the SSI- COV technique utilises the output covariance matrix or correlation as the mean of the signals is assumed to be zero. Both the SSI-DATA and SSI-COV techniques identify the state space models on the basis of the output measurements by using robust numerical techniques, such as singular value decomposition [6-7]. Once the state space model is determined, it is straightforward to extract natural frequencies from the stabilisation diagram, as shown in Fig. 4, and also to produce the associated damping ratios and mode shapes.

The identified frequencies from the known data for case S1-S13 by both the SSI-DATA and SSI-COV techniques are summarised in Table 2 and Table 3, respectively. The identified frequencies range between 0.15Hz and 0.40Hz. In the typhoon condition (S7 to S10), all the identified first eight frequencies are almost the same as the results of Ni et al. (2015) [19]. However, in the weak wind condition (S1 to S6), the second and the fifth frequencies can not be identified in this study. When the wind speed is around 7.5m/s (S11 to S13), the second frequencies are clearly identified in all data samples using both SSI-DATA and SSI-COV techniques. However, there are some frequencies in certain data samples cannot be identified using SSI-DATA or SSI-COV technique, e.g. the 3rd frequency in sample 11 and the 5th frequency in sample S13 using SSI-DATA, the 3rd frequency in sample S11 and the 5th frequency in samples S12 and S13 using SSI-COV.

The stabilisation diagrams for three typical data samples (S2, S7 and S12) using both the SSI-DATA and SSI-COV techniques are shown in Fig. 4. From the results, the stabilisation diagrams are different under various wind speed conditions, which can be used for a qualitative judgement on the excitation levels. In the typhoon condition (S7), the identified 8 frequencies are clearly indicated on the stabilisation diagrams, as shown in Fig. 4(c) and 4(d). In the weak wind condition (S2), the second and the fifth frequencies are not shown on the stabilisation diagrams, as given in Fig. 4(a) and 4(b). In the condition when the wind speed is around 7.5m/s (S12), the stabilisation diagrams shown in Fig. 4(e) and 4(f), are not as good as those under the typhoon condition. However the frequencies are still shown on the stabilisation diagrams except the fifth frequency on the stabilisation diagram using SSI-COV technique, as shown in Fig. 4(f).

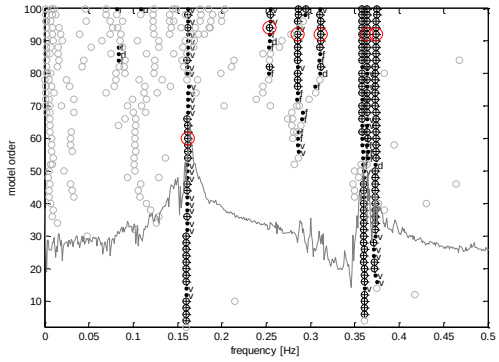

(a) Case S2 using SSI-DATA

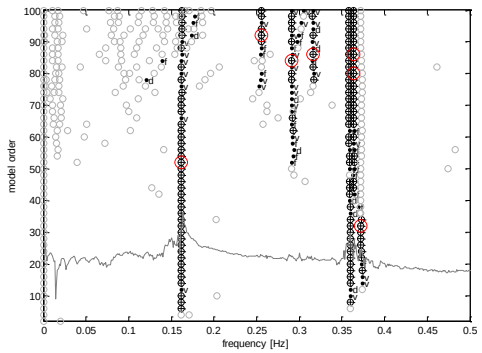

(b) Case S2 using SSI-COV

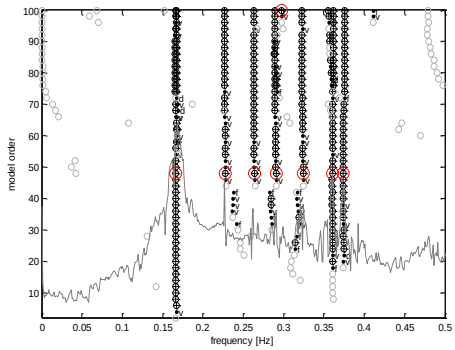

(c) Case S7 using SSI-DATA

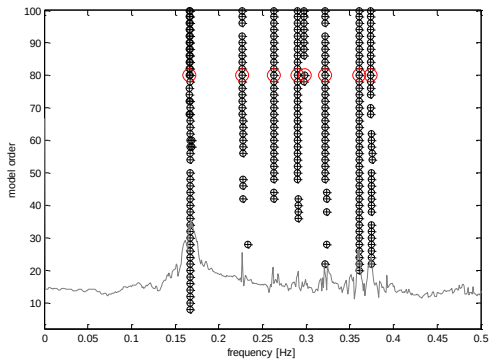

(d) Case S7 using SSI-COV

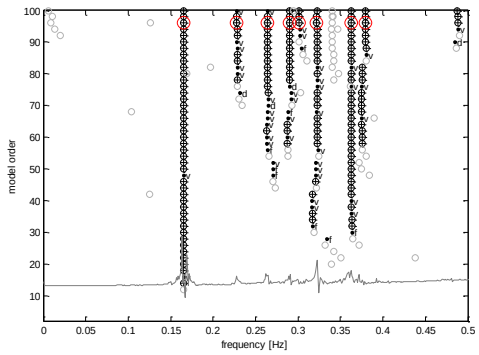

(e) Case S12 using SSI-DATA

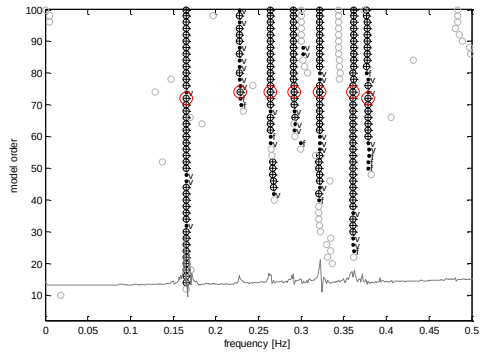

(f) Case S12 using SSI-COV

Fig. 4 The stabilisation diagrams for three typical data samples using both the SSI-DATA and SSI-COV techniques

Table 2 Identified frequencies (Hz) of the first 8 modes under different wind speed conditions using SSI-DATA technique

Mode No.	Weak wind						Typhoon				Wind speed around 7.5m/s		
	S1	S2	S3	S4	S5	S6	S7	S8	S9	S10	S11	S12	S13
1	0.161	0.161	0.161	0.165	0.165	0.165	0.167	0.164	0.164	0.164	0.168	0.165	0.168
2	-	-	-	-	-	-	0.228	0.228	0.227	0.227	0.228	0.228	0.226
3	0.254	0.254	0.256	0.256	0.255	0.259	0.264	0.264	0.260	0.260	-	0.264	0.265
4	0.286	0.286	0.283	0.285	0.282	0.284	0.291	0.292	0.287	0.287	0.282	0.290	0.291
5	-	-	-	-	-	-	0.298	0.301	0.297	0.297	0.301	0.301	-
6	0.307	0.311	0.304	0.313	0.311	0.317	0.324	0.324	0.319	0.319	0.315	0.322	0.323
7	0.358	0.364	0.360	0.359	0.357	0.358	0.361	0.361	0.358	0.358	0.361	0.363	0.366
8	0.372	0.374	0.374	0.372	0.371	0.373	0.374	0.374	0.375	0.374	0.376	0.380	0.377

Table 3 Identified frequencies (Hz) of the first 8 modes under different wind speed conditions using SSI-COV technique

Mode No.	Weak wind						Typhoon				Wind speed around 7.5m/s		
	S1	S2	S3	S4	S5	S6	S7	S8	S9	S10	S11	S12	S13
1	0.162	0.162	0.163	0.164	0.164	0.165	0.166	0.164	0.165	0.166	0.168	0.165	0.169
2	-	-	-	-	-	-	0.227	0.227	0.227	0.226	0.228	0.229	0.227
3	0.255	0.256	0.258	0.257	0.253	0.260	0.263	0.264	0.259	0.260	-	0.264	0.265
4	0.289	0.291	0.289	0.289	0.287	0.289	0.290	0.293	0.287	0.289	0.282	0.292	0.291
5	-	-	-	-	-	-	0.298	0.301	0.297	0.302	0.303	-	-
6	0.309	0.316	0.313	0.316	0.316	0.320	0.322	0.323	0.319	0.317	0.315	0.322	0.323
7	0.358	0.364	0.360	0.359	0.357	0.358	0.361	0.361	0.358	0.359	0.360	0.361	0.360
8	0.373	0.372	0.373	0.373	0.371	0.373	0.374	0.372	0.374	0.373	0.374	0.379	0.377

4. Modal contribution index for mode identifiability

On the basis of the SSI-DATA method, the modal contribution indexes of all identified modes to the measured vibration data are computed by using the Kalman filter, and their feasibility to evaluate the robustness of identified modes is also investigated here.

4.1 Modal contribution index

Given the measured accelerations, the state space model matrices can be estimated by using the SSI-DATA technique. Modal parameters can be directly extracted from the model matrices. A procedure to estimate the acceleration from individual identified modes using the Kalman filter by the model matrices has been proposed by Cara et al [26].

For an n_d degree-of-freedom (DOF) structure with proportional damping, the acceleration response of DOF *n*, a_n, can be expressed as the superposition of modal acceleration of all n_d modes

$$a_n = a_n^{m_1} + a_n^{m_2} + \cdots + a_n^{m_{n_d}}, n = 1, 2, \cdots n_d \tag{1}$$

where a_n is the acceleration response of DOF *n*; $a_n^{m_{n_d}}$ is the n_d-th theoretical modal acceleration of DOF *n*. The theoretical modal accelerations of all DOFs can be determined by using the mode-superposition method.

According to the proposed procedure by Cara et al [26], the modal accelerations of all DOFs can be estimated using the Kalman filter, namely

$$a_n \approx a_n^{k_1} + a_n^{k_2} + \cdots + a_n^{k_{n_d}}, n = 1, 2, \cdots n_d \tag{2}$$

where $a_n^{k_{n_d}}$ is the n_d-th estimated modal acceleration of DOF *n*. The research on an 8 DOF structure under white noise excitation shows that the theoretical modal accelerations are almost the same as the estimated modal accelerations [26].

By introducing the inevitable error between the theoretical and estimated modal accelerations using Kalman filter method a_n^{ε}, the acceleration response of DOF *n* is now expressed as

$$a_n = a_n^{k_1} + a_n^{k_2} + \cdots + a_n^{k_{n_d}} + a_n^{\varepsilon'} = a_n^{k'} + a_n^{\varepsilon'}, n = 1, 2, \cdots n_d \tag{3a}$$

where $a_n^{k'}$ is the estimated acceleration of DOF *n*; $a_n^{\varepsilon'}$ is the error between the theoretical and estimated acceleration of DOF *n.* For large civil engineering structures with infinite DOFs, only few lower order modes can be identified from the measurements, and then the corresponding modal accelerations can be estimated. Here the number of identified modes n_m ($n_m < n_d$) is assumed to be identified. Then Equation (3a) is rewritten as

$$a_n = a_n^{k_1} + a_n^{k_2} + \cdots + a_n^{k_{n_m}} + a_n^{\varepsilon} = a_n^{k} + a_n^{\varepsilon}, n = 1, 2, \cdots n_m \tag{3b}$$

Assuming a total n_o number of measurement locations with *N* data points, where n_o is normally less than the total number of DOF n_d, the measured accelerations can be expressed as the superposition of estimated accelerations and error. Rearranging these accelerations in the following matrix form,

$$\begin{bmatrix} a_{11} & a_{12} & \cdots & a_{1N} \\ a_{21} & a_{22} & \cdots & a_{2N} \\ \vdots & \vdots & \vdots & \vdots \\ a_{n_o 1} & a_{n_o 2} & \cdots & a_{n_o N} \end{bmatrix}_{n_o \times N} = \begin{bmatrix} a_{11}^k & a_{12}^k & \cdots & a_{1N}^k \\ a_{21}^k & a_{22}^k & \cdots & a_{2N}^k \\ \vdots & \vdots & \vdots & \vdots \\ a_{n_o 1}^k & a_{n_o 2}^k & \cdots & a_{n_o N}^k \end{bmatrix}_{n_o \times N} + \begin{bmatrix} a_{11}^{\varepsilon} & a_{12}^{\varepsilon} & \cdots & a_{1N}^{\varepsilon} \\ a_{21}^{\varepsilon} & a_{22}^{\varepsilon} & \cdots & a_{2N}^{\varepsilon} \\ \vdots & \vdots & \vdots & \vdots \\ a_{n_o 1}^{\varepsilon} & a_{n_o 2}^{\varepsilon} & \cdots & a_{n_o N}^{\varepsilon} \end{bmatrix}_{n_o \times N} \tag{4}$$

$$\Rightarrow \boldsymbol{A} = \boldsymbol{A}^k + \boldsymbol{A}^{\varepsilon}$$

Multiplying by the transpose of $\boldsymbol{A}$ and retaining only the diagonal elements, gives

$$\boldsymbol{A}\boldsymbol{A}^T = \boldsymbol{A}^k\boldsymbol{A}^T + \boldsymbol{A}^\varepsilon\boldsymbol{A}^T \tag{5}$$

$$\left(\boldsymbol{A}\boldsymbol{A}^T\right)_D = \left(\boldsymbol{A}^k\boldsymbol{A}^T\right)_D + \left(\boldsymbol{A}^\varepsilon\boldsymbol{A}^T\right)_D \tag{6}$$

where $(\bullet)_D$ is the diagonal operator, i.e. giving a matrix only consisting of the diagonal elements of the matrix and zeros elsewhere. Normalising Eq. (6) gives

$$\begin{aligned}&\left(\boldsymbol{A}\boldsymbol{A}^T\right)_D^{-1}\left(\boldsymbol{A}\boldsymbol{A}^T\right)_D = \left(\boldsymbol{A}\boldsymbol{A}^T\right)_D^{-1}\left(\boldsymbol{A}^k\boldsymbol{A}^T\right)_D + \left(\boldsymbol{A}\boldsymbol{A}^T\right)_D^{-1}\left(\boldsymbol{A}^\varepsilon\boldsymbol{A}^T\right)_D \\ &\Rightarrow \{1\}_{n_o} = \boldsymbol{\Delta}_k + \boldsymbol{\Delta}_\varepsilon\end{aligned} \tag{7}$$

where $\{1\}_{n_o}$ is a column vector with n_o elements of a single value of unity; $\boldsymbol{\Delta}_k$ and $\boldsymbol{\Delta}_\varepsilon$ are column vectors representing the diagonal of matrix $\left(\boldsymbol{A}\boldsymbol{A}^T\right)_D^{-1}\left(\boldsymbol{A}^k\boldsymbol{A}^T\right)_D$ and $\left(\boldsymbol{A}\boldsymbol{A}^T\right)_D^{-1}\left(\boldsymbol{A}^\varepsilon\boldsymbol{A}^T\right)_D$, respectively.

According to Eq. (7), the element *i* of vector $\boldsymbol{\Delta}_k(i)$ and $\boldsymbol{\Delta}_\varepsilon(i)$, where $i = 1, 2, \cdots, n_o$ are defined as the contribution of the identified modes and the associated contribution of the error to the vibration measurement *I*, respectively. The total contribution of both the modes and the error is equal to unity in each measurement. In addition, the global contribution of the modes δ_k and the global contribution of the error δ_ε are defined as the mean value of the corresponding vector, respectively

$$\delta_k = \frac{1}{n_o}\sum_{i=1}^{n_o}\boldsymbol{\Delta}_k(i) \quad , \quad \delta_\varepsilon = \frac{1}{n_o}\sum_{i=1}^{n_o}\boldsymbol{\Delta}_\varepsilon(i) \quad \Rightarrow \delta_k + \delta_\varepsilon = 1 \tag{8}$$

Using Eq. (3b), the measurement matrix $\boldsymbol{A}$ can be expressed as the superposition of the estimated modes and the error

$$\boldsymbol{A} = \boldsymbol{A}^{k_1} + \boldsymbol{A}^{k_2} + \cdots + \boldsymbol{A}^{k_{n_m}} + \boldsymbol{A}^\varepsilon \tag{9}$$

By using the same procedure, leading to

$$\{1\}_{n_o} = \left(\boldsymbol{A}\boldsymbol{A}^T\right)_D^{-1}\left(\boldsymbol{A}^{k_1}\boldsymbol{A}^T\right)_D + \left(\boldsymbol{A}\boldsymbol{A}^T\right)_D^{-1}\left(\boldsymbol{A}^{k_2}\boldsymbol{A}^T\right)_D + \cdots\left(\boldsymbol{A}\boldsymbol{A}^T\right)_D^{-1}\left(\boldsymbol{A}^{k_{n_m}}\boldsymbol{A}^T\right)_D + \left(\boldsymbol{A}\boldsymbol{A}^T\right)_D^{-1}\left(\boldsymbol{A}^\varepsilon\boldsymbol{A}^T\right)_D \tag{10}$$

Retaining only the diagonal of the matrices gives

$$\{1\}_{n_o} = \boldsymbol{\Delta}_{k_1} + \boldsymbol{\Delta}_{k_2} + \cdots + \boldsymbol{\Delta}_{k_{n_m}} + \boldsymbol{\Delta}_\varepsilon \tag{11}$$

$$\delta_{k_j} = \frac{1}{n_o}\sum_{i=1}^{n_o}\boldsymbol{\Delta}_{k_j}(i) \quad \Rightarrow \quad \sum_{j=1}^{n_m}\delta_{k_j} + \delta_\varepsilon = \delta_k + \delta_\varepsilon = 1 \tag{12}$$

where $\boldsymbol{\Delta}_{k_j}(i)$ is the contribution of the identified mode *j* to the measurement *i*; δ_{k_j} is the contribution of the identified mode *j* to the total measurement.

4.2 Estimated modal contribution index value

For the present benchmark study, the number of measured accelerations is the number of uni-axial accelerometers installed on the bridge deck, i.e., $n_o = 24$. The duration of the acceleration data is 1 hour and the sampling frequency is 25.6 Hz, giving the data points *N* of 92,160. From the results in Table 2 and Table 3, the frequency range of interest lies between 0.1 and 0.5 Hz, containing at least the first 8 frequencies within this range. A filtering using the 8th order Chebyshew Type I band-pass digital filter within 0.1 to 0.5Hz and resampling from 25.6 to 2.56 Hz are performed for these measured data, leading to 9,216 data points with a frequency range from 0.1 to 0.5Hz.

The modal contribution indexes of the identified modes to the total measurements for S1 to S13 are estimated and summarised in Table 4. The modal contribution indexes for three typical data samples (S2, S7 and S12) are also shown in Fig. 5 for more detailed illustration.

As shown in Fig. 5(a) and Table 4, in the weak wind conditions, the total modal contribution index of all identified 6 modes are less than 0.670 and the mean value is 0.635, which means that the contribution of the identified modes is lower, and approximately 37.5% of the total measured acclamations are noise and estimated error. The contributions of the 2nd and 5th modes to the total measurement are so small that they can not be identified in this excitation level.

In the typhoon conditions, as shown in Fig. 5(b) and Table 4, the total modal contribution index of all identified 8 modes are more than 0.810 and the mean value is 0.836, indicating that the contribution of the modes is much higher and only around 16.4% of the total measured acclamations are noise and estimated error. For the 2nd mode that was not identified in the weak wind conditions, it can be seen that their contributions to the total measurement are more than 3.7% in the typhoon conditions. It could be the reason why they can be clearly identified in the typhoon conditions. For the 5th mode, their contributions to the total measurements are only around 1%. Although it can be identified, the robustness may not be stable.

When the speed wind is around 7.5m/s, the value of total modal contribution index of all identified modes are higher than the values in the weak wind conditions and even higher than the values in the typhoon conditions in some cases such as S12, as shown in Fig. 5(c) and Table 4. The mean value for this wind condition is 0.787. For the 2nd mode, its contribution to the total measurement is more than 2.2%, making it clearly identifiable. For the 5th mode, its contribution to the total measurement is less than 1%, which is still identifiable. However, its robustness may be weak. In addition, the 3rd mode in case S11 and the 5th mode in case S13 cannot be identified due to their very low contributions to the total measurements.

In summary, as wind speed becomes higher, more modes will be excited and identified, since their contributions to the total measurement will be higher. The mode identifiability may not be only related to the ambient excitation intensity, but also depends on their modal contributions to the measured vibration data. The critical value of modal contribution index for a reliable and robust identified mode is suggested as at least 2% for this benchmark problem.

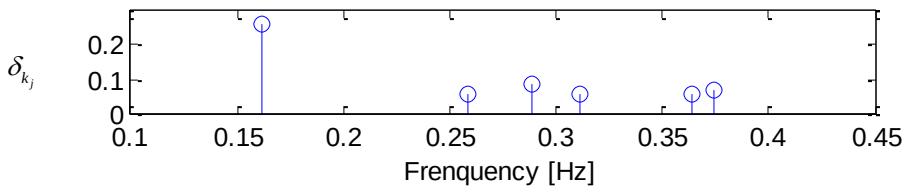

(a) S2 (δ_k =0.577)

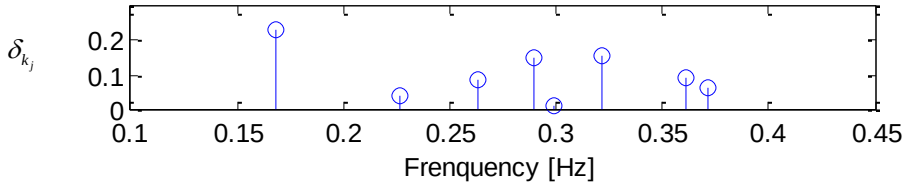

(b) S7 (δ_k =0.820)

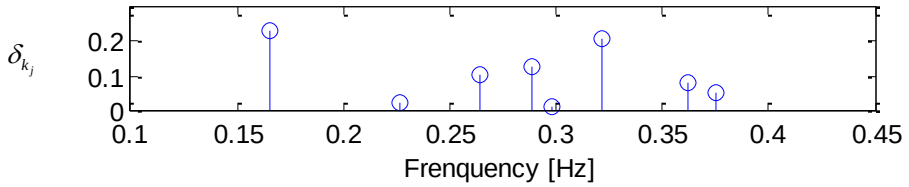

(c) S12 (δ_k =0.829)

Fig. 5 The modal contribution indexes of the identified modes to the total measurement for three typical data samples (S2, S7 and S13)

Table 4 Modal contribution indexes for identified modes to the total measurements

Mode No.	Weak wind						Typhoon				Wind speed around 7.5m/s		
	S1	S2	S3	S4	S5	S6	S7	S8	S9	S10	S11	S12	S13
1	0.260	0.260	0.237	0.266	0.213	0.238	0.233	0.195	0.191	0.160	0.232	0.232	0.182
2	-	-	-	-	-	-	**0.039**	**0.037**	**0.040**	**0.074**	**0.061**	**0.022**	**0.064**
3	0.068	0.054	0.080	0.087	0.055	0.103	0.084	0.090	0.044	0.062	-	0.102	0.083
4	0.082	0.085	0.064	0.082	0.072	0.048	0.148	0.118	0.104	0.148	0.063	0.125	0.225
5	-	-	-	-	-	-	**0.008**	**0.006**	**0.014**	**0.008**	**0.008**	**0.009**	**-**
6	0.058	0.054	0.053	0.045	0.051	0.049	0.155	0.109	0.124	0.252	0.055	0.206	0.185
7	0.117	0.057	0.113	0.114	0.153	0.149	0.090	0.150	0.181	0.105	0.218	0.082	0.032
8	0.074	0.067	0.080	0.075	0.069	0.077	0.063	0.149	0.112	0.048	0.093	0.051	0.027
Total	**0.660**	**0.577**	**0.627**	**0.668**	**0.613**	**0.664**	**0.820**	**0.856**	**0.811**	**0.857**	**0.730**	**0.829**	**0.803**
Mean			**0.635**					**0.836**				**0.787**	

5. Mode identifiability on the blind data samples

The identified frequencies from the six data samples with unknown wind condition by using both the SSI-DATA and SSI-COV techniques are summarised in Table 5. The identified frequencies are all within the range between 0.15Hz and 0.40Hz. For the case S14, S15 and S17, all the first 8 frequencies can be clearly identified, which is the same as the Typhoon condition. For the cases S18 and S19, the 2nd and the 5th frequencies cannot be identified, which is the same as the weak wind condition. For the case S16, only the 3rd frequency cannot be identified, which is probably the critical condition. Based on the analysis on these identified frequencies, it can be preliminarily concluded that cases S14, S15 and S17 are in the Typhoon condition, cases S18 and S19 are in the weak wind condition, and case S16 is in the condition with wind speed of around 7.5m/s. As shown in Fig. 6, the stabilisation diagrams for three data samples (S14, S16 and S18) using both the SSI-DATA and SSI-COV techniques can be further used to confirm the preliminary conclusions.

Table 5 Identified frequencies (Hz) of the first 8 modes from the blind data using SSI-DATA and SSI-COV techniques

Mode No.	SSI-DATA						SSI-COV					
	S14	S15	S16	S17	S18	S19	S14	S15	S16	S17	S18	S19
1	0.168	0.168	0.164	0.166	0.162	0.161	0.169	0.169	0.165	0.166	0.163	0.162
2	0.227	0.228	0.229	0.229	-	-	0.227	0.228	0.228	0.229	-	-
3	0.264	0.264	-	0.262	0.256	0.252	0.265	0.264	-	0.262	0.258	0.254
4	0.291	0.291	0.283	0.293	0.285	0.280	0.291	0.291	0.283	0.293	0.290	0.287
5	0.300	0.303	0.301	0.303	-	-	0.303	0.300	0.305	0.305	-	-
6	0.323	0.322	0.314	0.321	0.307	0.311	0.322	0.321	0.321	0.320	0.312	0.316
7	0.362	0.361	0.357	0.360	0.359	0.360	0.361	0.360	0.358	0.359	0.359	0.360
8	0.379	0.376	0.373	0.375	0.374	0.374	0.376	0.373	0.372	0.374	0.373	0.373

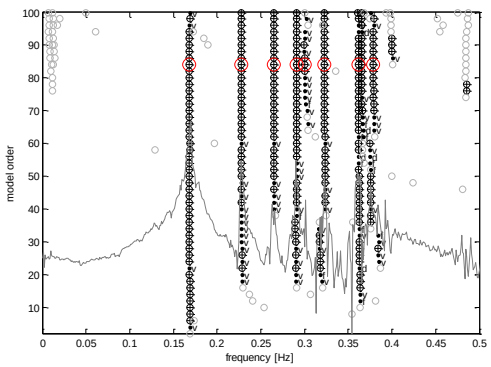

(a) Case S14 using SSI-DATA

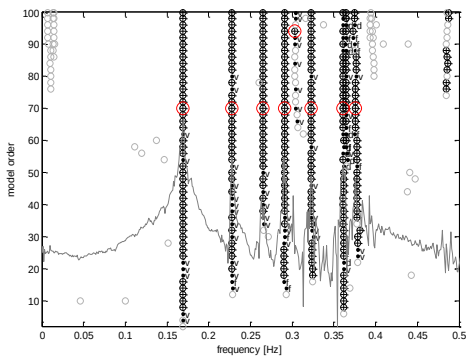

(b) Case S14 using SSI-COV

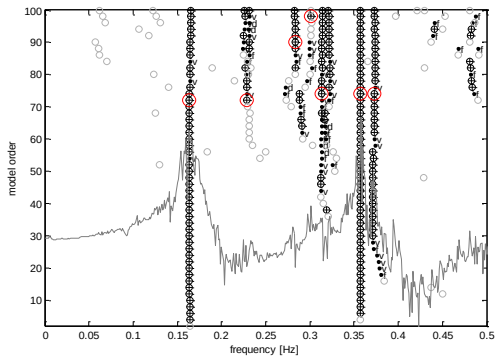

(c) Case S16 using SSI-DATA

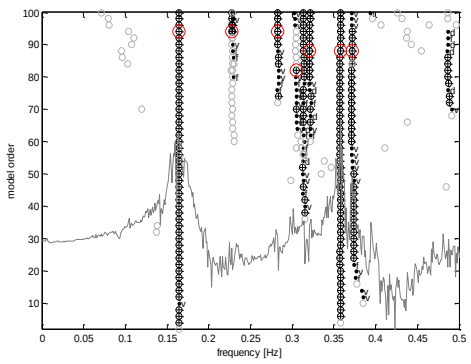

(d) Case S16 using SSI-COV

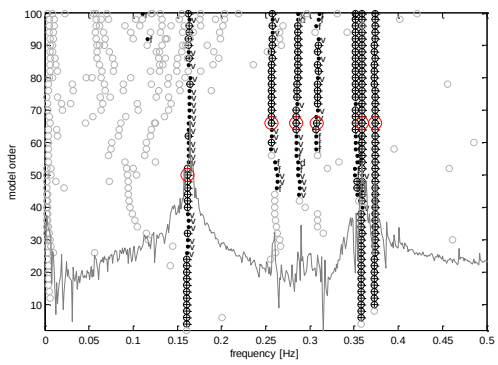

(e) Case S18 using SSI-DATA

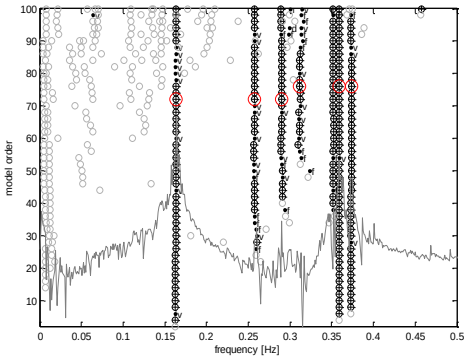

(f) Case S18 using SSI-COV

Fig. 6 The stabilisation diagrams for three data samples (S14, S16 and S18) using both the SSI-DATA and SSI-COV techniques

To further validate the preliminary conclusions, the modal contribution indexes of the identified modes to the total acceleration measurements for S14 to S19 are estimated and summarised in Table 6. The modal contribution indexes of the identified modes to the total measurements for three typical data samples (S14, S16 and S18) are shown in Fig. 6.

For cases S14, S15 and S17, as shown in Fig. 6(a) and Table 6, the total modal contribution indexes of all identified 8 modes are 0.828, 0.819 and 0.825, respectively, which are almost the same as those for S7 to S10. The stabilisation diagram in Fig. 6(a) is also similar to Fig. 4(c). It may be rationally concluded that cases S14, S15 and S17 are in the typhoon condition.

For case S16, the total modal contribution index of all identified modes are 0.722 and the 3rd frequency cannot be identified, as shown in Fig. 6(b) and Table 6. All these results are almost the same as those for the case S11. It can be rationally concluded that case S16 is in the critical condition.

For cases S18 and S19, the total modal contribution indexes of all identified 6 modes are 0.682, which is almost the same as those for S1 to S6, as shown in Fig. 6(c) and Table 6. The stabilisation diagram in Fig. 6(c) is also similar to Fig. 4(a). In addition, the contributions of the 2nd and 5th modes to the total measurement are also too low to be identified in this excitation level. It can be rationally concluded that cases S18 and S19 are in the weak wind condition.

Table 6 Modal contribution index value for identified modes to the total measurements

Mode No.	Modal contribution index value					
	S14	S15	S16	S17	S18	S19
1	0.218	0.207	0.240	0.224	0.241	0.241
2	0.073	0.046	**0.045**	**0.018**	-	-
3	0.066	0.088	-	0.100	0.085	0.085
4	0.221	0.134	0.074	0.117	0.072	0.072
5	0.011	0.009	**0.011**	**0.015**	-	-
6	0.157	0.192	0.088	0.200	0.061	0.061
7	0.036	0.038	0.182	0.093	0.154	0.154
8	0.047	0.106	0.082	0.057	0.070	0.070
total	**0.828**	**0.819**	**0.722**	**0.825**	**0.682**	**0.682**

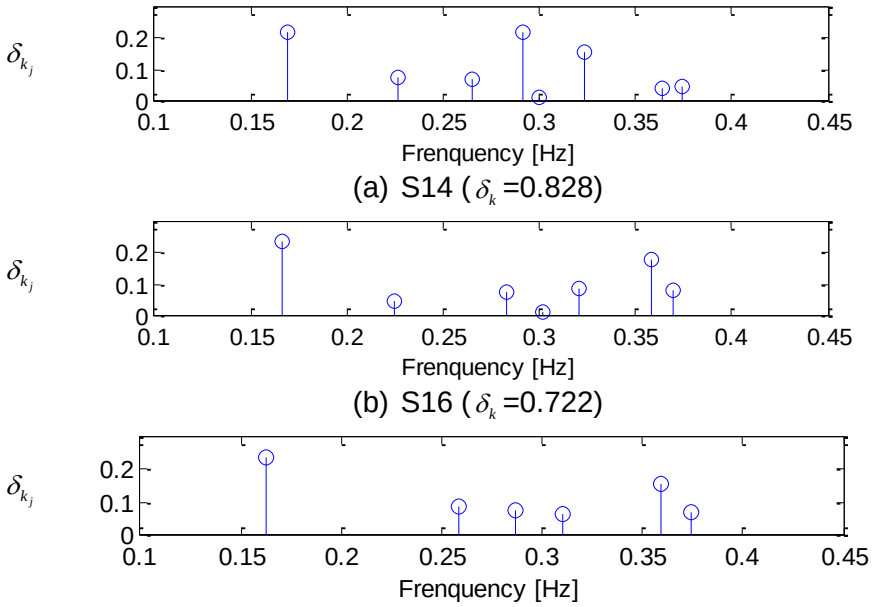

(a) S14 (δ_k =0.828)

(b) S16 (δ_k =0.722)

(c) S18 (δ_k =0.682)

Fig. 6 Modal contribution indexes of the identified modes to the total acceleration measurements for three typical data samples (S14, S16 and S18)

6. Conclusions

This study presents an in-depth investigation on a benchmark problem about the mechanism on the mode identifiability of a cable-stayed bridge using real monitored acceleration data under different excitation conditions. Two time-domain OMA methods, the SSI-DATA and SSI-COV techniques, are adopted to identify the modal parameters from ambient acceleration measurements. A modal contribution index measuring the contribution of identified mode to the measured vibration data using the Kalman filter is proposed to evaluate the robustness of identified modes. This benchmark study shows that the mode identifiability is not only related to the ambient excitation intensity, but also depended on their modal contributions to the measured vibration data. A critical value of modal contribution index for a reliable and robust identified mode is suggested as 2%.

It should be noted that the identified modal parameters may be affected not only by the excitation intensity (e.g. the magnitude of wind speed), but also by the excitation sources (e.g. wind and traffic) and the excitation direction (e.g. the wind directions) etc. The modal contribution index should be used to assess the robustness of the identified modes, together with other methods.

Acknowledgments

The authors greatly appreciate Prof. Y.Q. Ni at Hong Kong Polytechnic University for providing the monitoring data and related materials on this research. The authors also thank the financial support granted by the UK Royal Academy of Engineering Newton Fund (Reference NRCP/1415/14), the Natural Science Foundation of China (Grant No. 51478472), the Natural Science Foundation of Hunan Province, China (Grant No. 2015JJ2176) and the China Scholarship Council (CSC No. 201506375059).

References

1. Ewins, D.J. (2000). Modal Testing: Theory, Practice and Application (2nd edition). Research Studies Press Ltd, Hertfordshire.
2. Bendat, J.S. and Piersol, A.G. (1993) “Engineering applications of correlation and spectral analysis”, New York, NY, Wiley-Interscience.
3. Brincker, R., Zhang, L., and Andersen, P. (2000). Modal identification from ambient responses using frequency domain decomposition. In: Proceedings of the 18th International Modal Analysis Conference (IMAC), San Antonio, Texas.
4. Guillaume, P., Verboven, P., Vanlanduit, S., Van Der Auweraer, H. and Peeters, B. (2003). A poly-reference implementation of the least-squares complex frequency-domain estimator. In: Proceedings of the 21st International Modal Analysis Conference (IMAC), Kissimmee, FL.
5. Juang, J. N. and Pappa, R. S. (1985). An eigensystem realization algorithm for modal parameter identification and model reduction. Journal of guidance, control, and dynamics, 8(5), 620-627.
6. Overschee, V.P. and De Moor, B. (1996). Subspace Identification for Linear Systems. Kluwer Academic Publisher, Dordrecht, The Netherlands.
7. Peeters, B. and De Roeck, G. (1999). Reference-based stochastic subspace identification for output-only modal analysis. Mechanical systems and signal processing, 13(6), 855-878.
8. Cunha, A., Caetano, E. and Delgado, R. (2001). Dynamic tests on large cable-stayed

bridge. Journal of Bridge Engineering, 6(1), 54-62.
9. Ren, W. X., Peng, X. L. and Lin, Y. Q. (2005). Experimental and analytical studies on dynamic characteristics of a large span cable-stayed bridge. Engineering Structures, 27(4), 535-548.
10. Magalhães, F., Cunha, A. and Caetano, E. (2008). Dynamic monitoring of a long span arch bridge. Engineering Structures, 30(11), 3034-3044.
11. Brownjohn, J. M. W., Magalhães, F., Caetano, E. and Cunha, A. (2010). Ambient vibration re-testing and operational modal analysis of the Humber Bridge. Engineering Structures, 32(8), 2003-2018.
12. Le, T.-H. and Caracoglia, L. (2015). High-order, closely-spaced modal parameter estimation using wavelet analysis. Structural Engineering and Mechanics, 56(3), 423-442.
13. Chen H.-P. (2006). Efficient methods for determining modal parameters of dynamic structures with large modifications. Journal of Sound and Vibration, 298(1-2), 462-470.
14. Arslan, M. E. and Durmuş, A. (2014). Modal parameter identification of in-filled RC frames with low strength concrete using ambient vibration. Structural Engineering and Mechanics, 50(2), 137-149.
15. Chen H.-P. and Maung T. S. (2014). Regularised finite element model updating using measured incomplete modal data. Journal of Sound and Vibration, 333(21), 5566–5582.
16. Chen, H.-P. and Huang, T.-L. (2012). Updating finite element model using dynamic perturbation method and regularization algorithm. Smart Structures and Systems, 10(4-5), 427-442.
17. Moradipour, P., Chan, T. H.T. and Gallage, C. (2015). An improved modal strain energy method for structural damage detection, 2D simulation. Structural Engineering and Mechanics, 54(1), 105-119.
18. Chen H.-P. and Maung T. S. (2014). Structural damage evolution assessment using regularised time step integration method. Journal of Sound and Vibration, 333(18), 4104–4122.
19. Ni, Y.Q., Wang, Y.W. and Xia, Y.X. (2015). Investigation of mode identifiability of a cable-stayed bridge: comparison from ambient vibration responses and from typhoon-induced dynamic responses. Smart Structures and Systems, 15(2), 447-468.
20. Zhang, F.-L. Yi-Qing Ni, Y.-Q. and Yan-Chun Ni, Y.-C. (2016). Mode identifiability of a cable-stayed bridge based on a Bayesian method. Smart Structures and Systems, 17(3), 471-489.
21. Goi Y. and Kim C.W. (2016). Mode identifiability of a multi-span cable-stayed bridge utilizing stabilization diagram and singular values. Smart Structures and Systems, 17(3), 391-411.
22. Magalhães, F. and Cunha, A. (2016). Automated identification of the modal parameters of a cable-stayed bridge: Influence of the wind conditions. Smart Structures and Systems, 17(3), 431-444.
23. Park, J.-H., Huynh, T.-C., Lee, K.-S. and Kim J.-T. (2016). Wind and traffic-induced variation of dynamic characteristics of a cable-stayed bridge – benchmark study. Smart Structures and Systems, 17(3), 491-522.
24. Ko, J. M. and Ni, Y. Q. (2005). Technology developments in structural health monitoring of large-scale bridges. Engineering structures, 27(12), 1715-1725.
25. Ni, Y. Q., Wong, K. Y. and Xia, Y. (2011). Health checks through landmark bridges to sky-high structures. Advances in Structural Engineering, 14(1), 103-119.
26. Cara, F. J., Juan, J., Alarcón, E., Reynders, E. and De Roeck, G. (2013). Modal contribution and state space order selection in operational modal analysis. Mechanical Systems and Signal Processing, 38(2), 276-298.